Volume 2
Number 5
September 2023
Pages 979–1324

Sensors & Diagnostics

rsc.li/sensors

ISSN 2635-0998

ROYAL SOCIETY OF CHEMISTRY

TUTORIAL REVIEW
Sankarasekaran Shanmugaraju *et al.*
Fluorescence sensing and bioimaging of Cu(II) ions using amino-1,8-naphthalimide-based small-molecule chemosensors

Sensors & Diagnostics

TUTORIAL REVIEW

View Article Online
View Journal | View Issue

Cite this: *Sens. Diagn.*, 2023, **2**, 1158

Fluorescence sensing and bioimaging of Cu(II) ions using amino-1,8-naphthalimide-based small-molecule chemosensors

Binduja Mohan, †
Noushija Mannanthara Kunhumon† and Sankarasekaran Shanmugaraju *

Fluorescence chemosensors for selective sensing and quantification of biologically important metal ions have attracted substantial research interest in recent years. Cu(II) is the third most abundant transition metal ion and an essential heavy metal ion present in the human body. Cu(II) plays many essential functions in living systems as a catalytic co-factor in various enzyme functions and electron transport. The alteration in the essential concentration of Cu(II) causes several deadly diseases like Menke's syndrome, Wilson's disease, and Alzheimer's disease. Given this, in the past decades, many small-molecule fluorescence sensors have been developed and employed for trace detection and monitoring the concentration of Cu(II) ions in biological systems. In particular, amino-1,8-naphthalimide fluorescence sensors have gained special research interest for Cu(II) sensing because of their facile synthesis, easy functional, structure tunability, and strong fluorescence emission in the visible region. In this article, we have discussed the applications of various amino-1,8-naphthalimide-based small-molecule fluorescence chemosensors for selective sensing and bioimaging of Cu(II) ions. In each section, we provide a detailed report on the synthesis, photophysics, and fluorescence sensing properties including bioimaging of amino-1,8-naphthalimide-small-molecule fluorescence chemosensors for Cu(II) ions.

Received 17th May 2023,
Accepted 5th July 2023

DOI: 10.1039/d3sd00115f

rsc.li/sensors

1. Introduction

The field of sensor chemistry has captured widespread global attention because of its relevance and significance in sensing biologically important and environmentally concerning analytes.[1] Metal ions play pivotal roles in the human body since metal ions are involved in various physiological processes.[2] Contamination of food and water due to industrial discharges, which majorly comprise heavy metal ions and other impurities, generates toxic effects on human health and adverse impact on the environment.[3] Metallic products have become part of our daily life in various forms

Department of Chemistry, Indian Institute of Technology Palakkad, Palakkad-678557, Kerala, India. E-mail: shanmugam@iitpkd.ac.in
† These authors contributed equally.

Binduja Mohan

Ms. Binduja Mohan is currently a Ph.D. student at the Indian Institute of Technology Palakkad. She completed her M.Sc. in Chemistry from St. Thomas College Palai and B.Sc. in Chemistry from B K College, Amalagiri. Her research interests are mainly coordination-driven supramolecular self-assembly, design of theragnostic agents, and sensor chemistry.

Noushija Mannanthara Kunhumon

Ms. Noushija Mannanthara Kunhumon is currently a Ph.D. student at the Indian Institute of Technology Palakkad. She completed her M.Sc. in Chemistry from Calicut University campus, Thenhippalam, and her B.Sc. in Chemistry from Government Victoria College Palakkad. Her research interests are small-molecule-based fluorescence chemosensors for biologically related analytes.

like utensils, cookware, deodorants, drinking water supplies, *etc.* which further facilitates the bioaccumulation of heavy metal ions in the human body apart from industrial drainage.[4] Aberrations in the normal levels of essential metal ions and intake of hazardous metal ions cause a wide range of diseases and permanent injuries to the organs like kidney failure, stomach ulcers, hypertension, bone lesions, lung dysfunction, and cardiovascular and neuro-disorders.[3,5] Therefore, maintaining tight control over the homeostasis of metal ions is of paramount interest to maintain proper health and environmental sustainability.

Cu(II) is considered an essential trace heavy metal nutrient and the third most abundant transition metal after Fe(II) and Zn(II) in the human body.[6] Cu(II) plays many indispensable roles like a catalytic cofactor, controlling enzyme functions, and being involved in electron transport.[7] The alteration in the uptake or consumption of Cu(II) levels in the human body could result in various deadly diseases like Menke's syndrome, Wilson's disease, and Alzheimer's disease.[8–10] Besides, long-term exposure and consumption of Cu(II) ions would result in liver and kidney failures.[11] Further, the excess amount of Cu(II) is highly lethal to microorganisms that are critical for a proper balance of an ecosystem. The Environmental Protection Agency (EPA) has stated that the highest permissible level of Cu(II) ions in drinking water must be less than 20 μM.[12] Given this, great research interest has existed in recent years to develop practically useful sensor systems with superior sensing properties for selective detection and sensitive determination of Cu(II) ions.

In the past decades, the application of chemosensors in numerous fields has received great attention due to the exceptional achievements acquired in the design and development of fluorescent chemosensors for tracking metal ion concentration in the environment and biological systems with excellent selectivity and sensitivity.[13,14] Other analytical techniques such as electrochemical detection, element analysis, inductively coupled plasma mass spectrometry (ICP-MS), spectrophotometry, and chromatography also gained remarkable accomplishments in metal sensing.[15–18] Nevertheless, a few challenges still exist in these methods, which include low accuracy, inadequate qualitative ability, and expensive, laborious, and time-consuming instrumentation which have restricted the widespread applications of these methods. In light of this, fluorescence-based sensing has gained incredible attention in the area of metal sensing due to its unique features like being cost-effective, having superior sensitivity, quick sensing response, easy operation, and a non-invasive detection process.[19,20]

The basic paradigm for fluorescence chemosensors is fluorophore–spacer–receptor, in which the most commonly used fluorophores are anthracene, carbazole, fluorescein, rhodamine, boron-dipyrromethene (BODIPY), coumarin, and pyrene.[21–25] Owing to the outstanding features such as facile synthesis, tunable structures and functions, and interesting photophysical properties including large Stokes shift, high photo-stability, relatively high quantum yield, and solvent-dependent emission characteristics, amino-1,8-naphthalimide (**Nap**) dyes have evolved as a favorite fluorophore and thus, a large number of fluorescence sensors have been developed and successfully employed for sensing different analytes.[3,26,27] Amino-1,8-naphthalimides (**Naps**) are a classical heterocyclic 'push–pull' class of fluorophores that absorb and emit in the visible region. **Nap** derivatives are generally highly emissive due to the efficient internal charge transfer (ICT) transition from the amino group to the electron-deficient imide moiety.[3,26] Moreover, the fluorescence emission intensity of **Naps** highly depends on the position of the amino group on the naphthalene unit. 3-Amino-based **Naps** are less emissive than 4-amino-based **Naps** due to the less efficient ICT transitions.[28] In addition to the fluorescence sensing application, **Naps** have been used in various other applications including as fluorescent markers in biology, theragnostic agents, anticancer drugs, light-emitting diodes, electroluminescent materials, molecular logic gates, medicinal analgesics, fluorescence switches, liquid crystal displays, and organic photoconductive materials.[24–27] Considering all these advantages, in recent years, a plethora of amino-1,8-naphthalimide (**Nap**)-based fluorescent chemosensors have been designed for efficient sensing of biologically relevant Cu(II) ions at low concentrations. The present review article provides a detailed report on the recent advances made in the use of **Nap**-based small-molecule chemosensors for fluorescence sensing and bioimaging of Cu(II) ions.

Sankarasekaran Shanmugaraju

Dr. Sankarasekaran Shanmugaraju received his B.Sc. and M.Sc. degrees in Chemistry from The American College, Madurai, and his Ph.D. degree with a gold medal for the best thesis in Inorganic Chemistry from the Indian Institute of Science (IISc), Bengaluru. In 2014, he moved to Trinity College Dublin, Ireland as an Irish Research Council (IRC) postdoctoral fellow. He is currently working as an associate professor at the Indian Institute of Technology Palakkad. His current research activities are in the area of supramolecular materials and sensor chemistry.

2. Amino-1,8-naphthalimide-based fluorescence chemosensors for Cu(II) ion detection

In this section, we have exemplified the design, synthesis, photophysical, and fluorescence sensing properties of several

Nap-based fluorescence chemosensors for the detection of Cu(II) ions. In 2017, Pu and co-workers developed a photoactive diarylethene-based amino-1,8-naphthalimide Schiff base (**Nap-1**) which showed excellent fluorescent sensing properties towards Cu(II) ions (Fig. 1A–D).[29] The presence of diarylethene makes **Nap-1** an efficient photochromic system due to its exceptional photo-switchable characteristic (Fig. 1A). **Nap-1** displayed an effective photo-isomerization on changing the excitation wavelength. At λ = 297 nm UV light irradiation, **Nap-1** displayed sharp color changes from colorless to orange along with the appearance of a new absorption band at λ = 475 nm which is due to the formation of the closed-ring isomer of **Nap-1**. Moreover, the initial strong ICT-based fluorescence emission of **Nap-1** gradually decreased with the increased Cu(II) concentration (Fig. 1B and C). A clear color change from green fluorescence to colorless was observed upon the addition of Cu(II) ions into the **Nap-1** solution (Fig. 1C inset). Interestingly, the addition of other metal ions did not cause any visual color changes (Fig. 1D). The fluorescence changes were found to be irreversible even after the addition of excess ethylenediaminetetraacetic acid (EDTA) solution. The binding constant (K_a) was estimated to be 3.13×10^4 L mol^{-1} and the limit of detection (LoD) was calculated to be 2.4×10^6 mol L^{-1}. Job's plot and mass spectrometry analysis demonstrated a 1 : 1 coordination complex formation between sensor **Nap-1** and Cu(II). These studies confirmed that **Nap-1** could be used as a potential colorimetric and fluorescence 'turn-off' sensor for selective and irreversible sensing of Cu(II) ions.

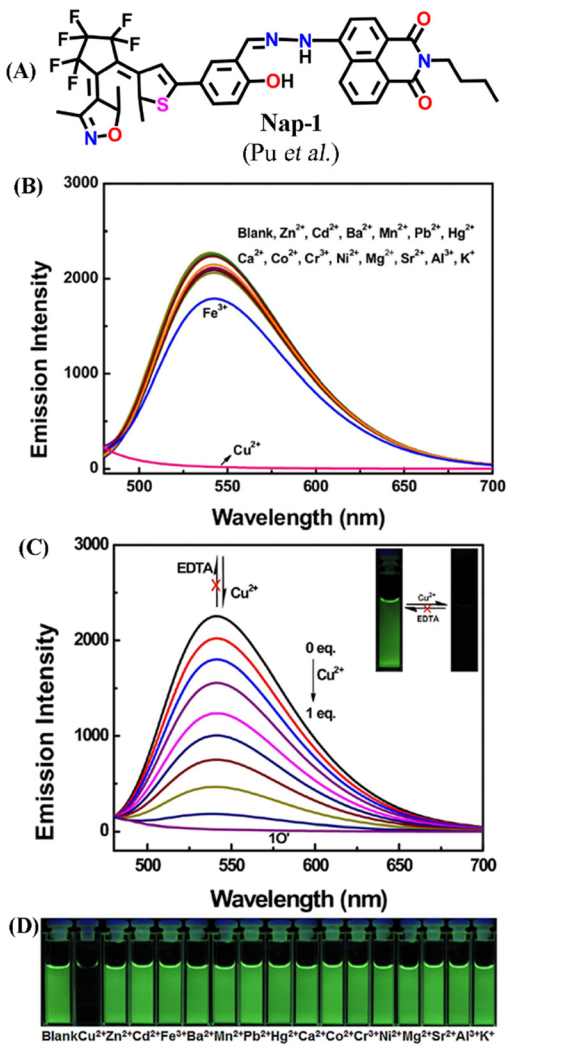

Fig. 1 (A) The structure of sensor **Nap-1**. (B) The observed changes in the fluorescence emission intensity of **Nap-1** were induced by various metal ions in CH_3CN. (C) The changes in fluorescence emission intensity of **Nap-1** induced by the addition of Cu(II) (inset: corresponding photographs of visual color changes). (D) Photographs for fluorescence color change of **Nap-1** in CH_3CN in the presence of various metal ions. Reproduced with permission from ref. 29. Copyright 2017 Elsevier.

A novel fluorescence chemosensor (**Nap-2**) based on an amino-1,8-naphthalimide having two [12]aneN$_3$ species for Cu(II) detection was reported (Fig. 2A–E).[30] **Nap-2** displayed an excellent 127-fold fluorescence quenching response with the incremental addition of Cu(II) ions and no notable inferences were seen with other competing metal cations including Ag(I), Cd(II), Ca(II), Fe(II), Co(II), Li(I), Hg(II), K(I), Ni(II), Mg(II), Na(I), Zn(II), and Pb(II) ions (Fig. 2B). The quantum yield of the **Nap-2** + Cu(II) coordination complex was much lower (ϕ = 0.0014) compared to sensor **Nap-2** (ϕ = 0.1498). Job's plot analysis confirmed that the binding stoichiometry between Cu(II) and **Nap-2** was 2 : 1. The detection limit in aqueous media was estimated to be 1.3×10^{-8} M which was much lower than the permissible limit of Cu(II) ions in drinking water. The amino-1,8-naphthalimide moiety with no [12]aneN$_3$ and triazole units exhibited no notable fluorescence alteration in the presence of Cu(II) ions. This data indicates that two [12]aneN$_3$ units are crucial for effective complex formation. The combined effect of the triazole-[12]aneN$_3$ unit and the amino-ester linkage resulted in the strong fluorescence quenching of **Nap-2** when coordinated with the Cu(II) ion. The non-radiative decay induced by the close contact between the amino-1,8-naphthalimide moiety and Cu(II) ion might be the reason for the attenuation in the fluorescence intensity. In addition, the complex Cu(II) + **Nap-2** could selectively detect adenosine triphosphate (ATP) which enhances the application of **Nap-2** in the biological field. Further, due to the increased biocompatibility, high water solubility, and good sensitivity for Cu(II) sensing, **Nap-2** was successfully used for the sequential sensing of Cu(II) and ATP both in an aqueous medium and within HeLa as well as A549 cells (Fig. 2D and E). The initial fluorescence intensity of **Nap-2** was diminished significantly after the addition of Cu(II) ions due to the efficient coordination complex formation, which was decomposed by the addition of ATP. The fluorescence intensity of **Nap-2** was restored by adding an increased concentration of ATP. At higher ATP concentrations, the HeLa and A549 cell lines exhibited a strong fluorescence emission and thus **Nap-2** can be used as a potential chemosensor for sensing and bioimaging of Cu(II).

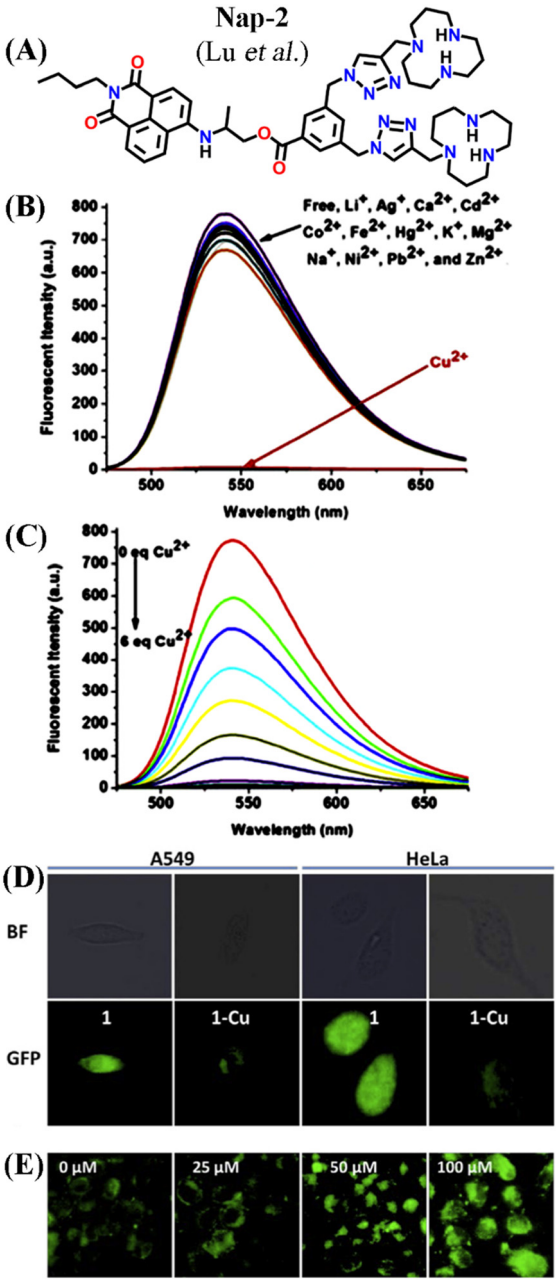

Fig. 2 (A) The structure of sensor **Nap-2**. (B) The observed relative changes in the fluorescence emission spectra of **Nap-2** were induced by various metal ions. (C) The changes in fluorescence emission intensity of **Nap-2** induced by the addition of Cu(II). (D) Confocal microscopy images of A549 and HeLa cells incubated with 10 μM **Nap-2** and **Nap-2** + Cu(II) for 1 h. (E) HeLa cells stained with 10 μM **Nap-2** + Cu(II) upon the addition of increasing concentration of ATP. Reproduced with permission from ref. 30. Copyright 2016 Elsevier.

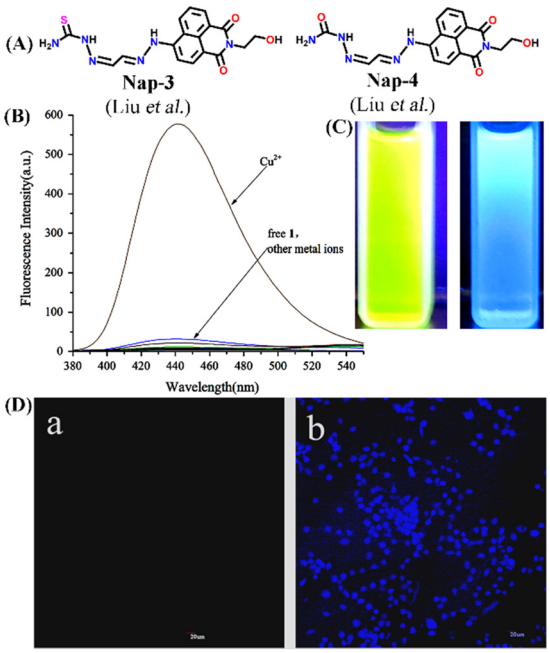

Fig. 3 (A) The structure of sensor **Nap-3** and **Nap-4**. (B) The relative changes in the fluorescence emission intensity of **Nap-3** were induced by various metal ions. (C) Visual color changes for **Nap-3** before and after binding with Cu(II) ions. (D) Fluorescence images of Hela cells incubated with **Nap-3** only (left-a) and **Nap-3** + Cu(II) for 1 h (right-b). Reproduced with permission from ref. 31. Copyright 2016 Elsevier.

In 2016, Liu *et al.* developed two interesting fluorescent sensors **Nap-3** and **Nap-4** for Cu(II) sensing (Fig. 3A and B) with the ability to display sharp visual color changes from yellow for **Nap-3** to blue upon Cu(II) binding (Fig. 3C).[31] The addition of Cu(II) ions into the **Nap-3** solution in CH_3CN/H_2O resulted in the decrease in emission intensity at λ = 530 nm which is accompanied by an unusual fluorescence enhancement at λ = 440 nm when excited at λ = 365 nm. The sensing properties of these sensors were stable in a wide range of pH and the addition of several competing metal ions did not show any changes in emission spectra (Fig. 3B). The reason for the exceptional enhancement of fluorescence intensity was ascribed to the strong coordination of the S atom to Cu(II) which suppresses the excited state fluorescence quenching of the amino-1,8-naphthalimide moiety. The binding ratio and limit of detection were determined to be 1 : 1 and 0.0326 μM. Interestingly, the subsequent addition of Na_2S reversed the fluorescence sensing through strong complex formation with Cu(II) ions. In addition to the fluorescence sensing, the ability of these sensors as cellular imaging probes was demonstrated using HeLa cells. The HeLa cells incubated with **Nap-3** did not show any fluorescence emission, but the addition of Cu(II) induced bright fluorescence emission (Fig. 3D). To support the proposed sensing mechanism, a reference sensor molecule **Nap-4** was designed, and similar titration studies were performed. Interestingly, the fluorescence titration showed significant fluorescence quenching with the appearance of no new peak, which suggested that "S" in **Nap-3** strongly coordinates to form a stable complex and thus efficient sensing. Therefore, **Nap-3** and **Nap-4** can be viewed as excellent fluorescence turn-on sensors for selective sensing and bioimaging of Cu(II) ions.

Another interesting **Nap**-based fluorescence sensor **Nap-5** with a Schiff base receptor was reported.[32] **Nap-5** is

composed of a **Nap** fluorophore unit directly connected with the Schiff base receptor without the spacer. **Nap-5** was highly fluorescent and displayed an excellent fluorescence quenching in the presence of Cu(II) ions in Tris-HCl buffer/DMF solution. The addition of other competing metal ions showed almost no observable changes in the emission intensity (Fig. 4A and B). The observed fluorescence quenching was due to the formation of a chelated, stable coordination complex between **Nap-5** and Cu(II). From the titration studies, the association constant and LoD were calculated to be 1.088×10^6 M^{-1} and 0.32 μM, respectively. In continuation, the same group reported another interesting sensor **Nap-6** with a slight modification at the receptor site.[33] Similar to **Nap-5**, sensor **Nap-6** also displayed an excellent fluorescence sensing ability for Cu(II), and no interference was observed in the presence of other competing ions at higher concentrations (Fig. 4C and D). The non-linear fitting curve and Job's plot analysis indicated that the binding ratio was 1 : 1 and the sensitivity of **Nap-6** for Cu(II) was 0.23 μM. These results confirm the effective sensing properties of **Nap-5** and **Nap-6** towards Cu(II) ions.

A novel fluorescence sensor **Nap-7** was designed by reacting 6-hydrazino-benzo[*de*]isoquinoline-1,3-diones with 4-*tert*-butyl-2,6-di-formyl phenol. **Nap-7** displayed a highly selective 30-fold fluorescence quenching response for Cu(II) in CH_3CN : H_2O (4 : 1, v/v) solution (Fig. 5A).[34] The high selectivity towards Cu(II) ions was not disturbed in the presence of other analytes including most of the alkali metals, alkaline earth metals and rare earth metals. The sensitivity was found to be as low as 64 ppb and this level of sensitivity is much lower than the allowed concentration of Cu(II) in water. The stoichiometry plot and ESI-MS analysis suggested that the binding ratio between **Nap-7** and the Cu(II) ion was 1 : 2. Notably, further studies using different salts of the Cu(II) ion such as $Cu(NO_3)_2$, $CuCl_2$, $Cu(ClO_4)_2$ and $Cu(OAc)_2$ showed no changes in the emission intensity and thus, the effect of anions on the sensing property of **Nap-7** was negligible. The observed fluorescence quenching was attributed to the photo-induced energy transfer from **Nap-7** to the Cu(II) ion and the high selectivity of **Nap-7** for Cu(II) was due to the strong affinity of heteroatoms (O and N) for Cu(II) and also to the ability of the Cu(II) ion to deprotonate the amide moiety. The selective fluorescence quenching for Cu(II) was also observed within the cellular medium (MCF-7 cells) with no apparent toxicity to the cell line (Fig. 5B). All these data affirm the excellent efficacy of **Nap-7** to act as a Cu(II) sensing probe both in solution and in the biological medium.

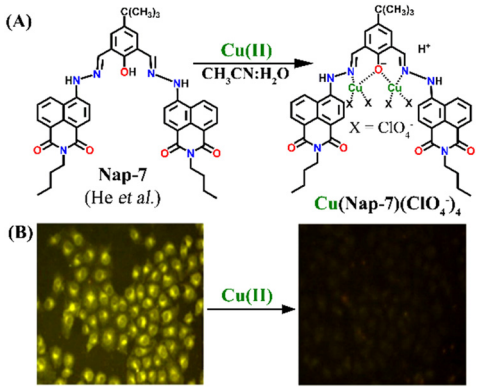

Fig. 5 (A) The structure of sensor **Nap-7** and its 1 : 2 complex formation with the Cu(II) ion in CH_3CN–H_2O solution. (B) The fluorescence microscopy image of **Nap-7** within MCF-7 cells before and after the addition of Cu(II) ions. Reproduced with permission from ref. 34. Copyright 2016 Elsevier.

In 2016, Zheng and his group reported a semicarbazide-based fluorescent sensor **Nap-8**, which showed a unique reaction-based turn-on fluorescence sensing towards Cu(II) ions.[35] The sensor **Nap-8** underwent a Cu(II) ion-promoted hydrolysis of the semicarbazide moiety into the formation of the corresponding amino-derivative which exhibited a strong fluorescence emission (see Fig. 6). The formation of the amino-derivative of **Nap-8** was verified based on the absorption and emission spectra recorded after the addition of Cu(II) in a buffer solution. Both the absorption and emission spectra matched well with already reported data for

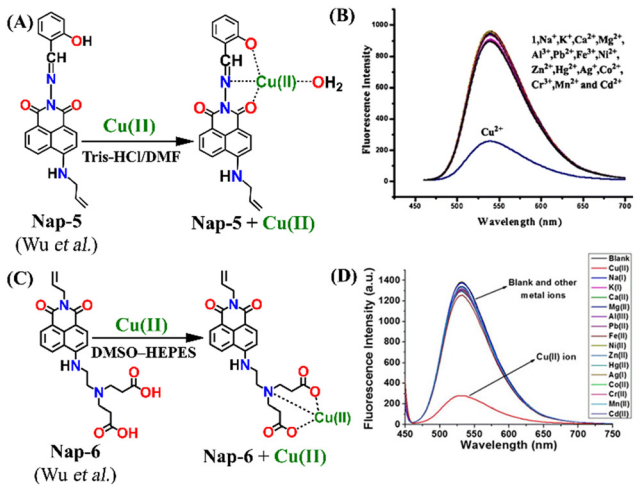

Fig. 4 The mechanism of Cu(II) sensing for (A) **Nap-5** and (C) **Nap-6**. The selectivity of the sensor (B) **Nap-5** and (D) **Nap-6** for Cu(II) ions in the co-existence of other competing metal ions. Reproduced with permission from ref. 32 and 33. Copyright 2017 Springer and 2017 Willey.

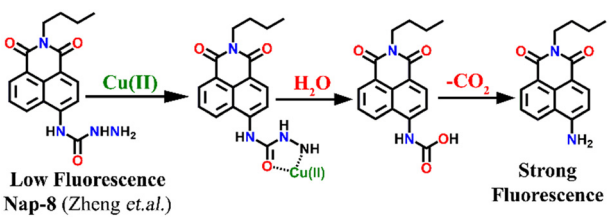

Fig. 6 The proposed reaction-based sensing mechanism of **Nap-8** for Cu(II) ions. The addition of Cu(II) induced hydrolysis to generate the amino-derivative of **Nap-8**.

the amino-derivative. The proposed hydrolysis-based sensing mechanism was further supported by the ESI-MS analysis. After the reaction of the Cu(II) ion with **Nap-8** in buffer medium, an intense peak at m/z = 269.3 was observed which corresponds to the proposed amino-derivative of **Nap-8**. This was further confirmed by multinuclear NMR (^{1}H and ^{13}C) analysis. Interestingly, **Nap-8** displayed an intense fluorescence enhancement even in the presence of other competing metal ions with excellent sensitivity and thus **Nap-8** can be used as an efficient fluorogenic chemo-dosimetry probe for the trace analysis of Cu(II) ions.

A novel fluorescence sensor (**Nap-9**) was synthesized *via* four-step reactions starting from 4-bromo-naphthalic anhydride.[36] The developed probe **Nap-9** displayed a highly selective and effective off–on type of fluorescence response for the addition of Cu(II) ions in CH_3CN–H_2O (70 : 30, v/v) along with a buffer solution of 3-(*N*-morpholino) propane sulfonic acid (MOPS, 10 mM, pH = 7.0) (Fig. 7A–C). The PET process from the electron-rich receptor moiety to the excited state of **Nap-9** fluorophore species was quenched in the presence of Cu(II) ions which eventually lead to the enhancement of fluorescence intensity (Fig. 7A). The fluorescence enhancement efficiency did not alter upon changing the concentration of Cu(II) ions from 1 to 10 equivalents, which indicates the binding stoichiometry as 1 : 1. This binding ratio was further confirmed using Job's plot analysis. The association constant was calculated to be 1.1 × 10^{10} M^{-1} and the LoD was 0.15 μM. The 4.5 fold fluorescence enhancement for **Nap-9** upon the addition of 10 equivalents of Cu(II) ion with no notable alteration with the presence of other metal analytes makes the sensor **Nap-9** an effective probe for Cu(II) ions (Fig. 7B and C).

Another interesting naphthalimide fluorescence sensor **Nap-10** adorned with a di-(2-picolyl)amino (DPA) receptor unit was reported for the excellent sensing of Cu(II) ions (Fig. 8A).[37] The absorption spectra of **Nap-10** displayed a clear hypochromic shift with the addition of Cu(II) ions which leads to a naked eye color change from a yellow shade to colorless. Interestingly, other metal ions did not show any notable shift in the absorption peak of the sensor. Similarly, the fluorescence emission intensity of **Nap-10** was altered significantly in the presence of Cu(II) ions. The initial strong emission of **Nap-10** was attenuated upon the addition of Cu(II) ion solution and this was also reflected by a marked color change (Fig. 8C and D). The bright green emission of **Nap-10** was observed to disappear after binding with the Cu(II) ion (Fig. 8C inset). The binding ratio between **Nap-10** and Cu(II) was estimated to be 1 : 1 by Job's plot. The electron-donating DPA receptor promotes a strong push–pull type of mechanism to the electron-withdrawing imide site which facilitates the strong internal charge transfer (ICT) transition. Upon metal binding, the lone pairs of electrons in the DPA moiety are no longer available for an efficient ICT process thus leading to the suppression of ICT which eventually resulted in the quenching of fluorescence. The

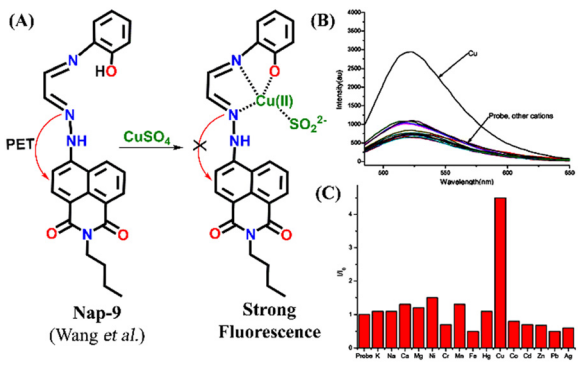

Fig. 7 (A) The structure of sensor **Nap-9** before and after the complex formation with the Cu(II) ion. (B) The relative changes in emission intensity observed for **Nap-9** after the addition of various metal ions and (C) their corresponding bar diagram showing the fluorescence turn-on response for the Cu(II) ion selectively. Reproduced with permission from ref. 36. Copyright 2013 Elsevier.

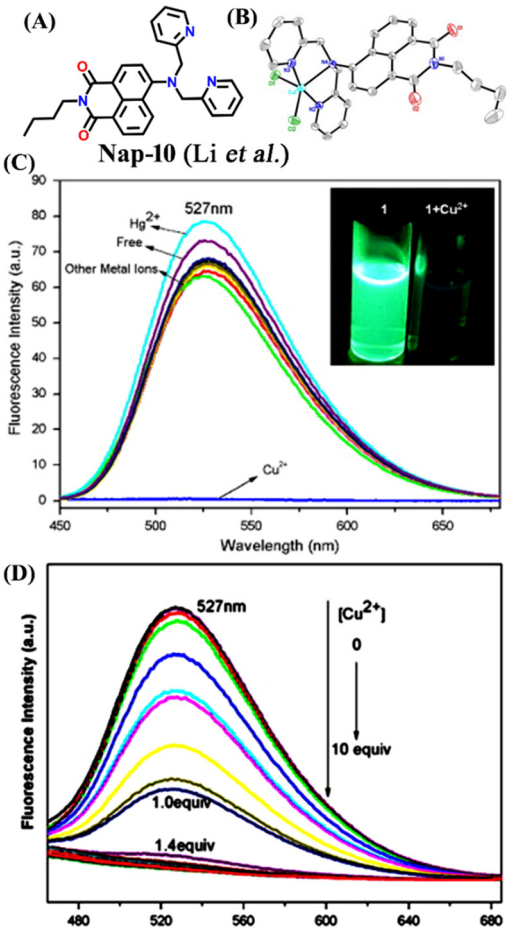

Fig. 8 (A) The structure of sensor **Nap-10** and (B) X-ray crystal structure of the 1 : 1 Cu(II) + **Nap-10** complex. (C) The relative changes in emission intensity before and after the addition of different metal cations [inset: color changes observed for **Nap-10** before and after the addition of Cu(II)]. (D) The changes in fluorescence emission intensity for **Nap-10** upon the gradual addition of Cu(II) ions. Reproduced with permission from ref. 37. Copyright 2012 Elsevier.

crystal structure of the Cu(II) + **Nap-10** complex reveals the Cu(II) coordination to three different nitrogen atoms, two of which belong to the pyridine ring unit and the other nitrogen from the naphthalene ring unit (Fig. 8B). The crystal data also validate the 1 : 1 binding ratio. The geometry of the complexation was observed to be trigonal bipyramidal. This is the first example of the successful crystal structure of the di-2-picoly-amine (DPA)–Cu(II) complex.

Tris-(2-aminomethyl)amine (tren) is a flexible amine used extensively in the design and synthesis of luminescent organic cages and organic polymers.[38] Due to its facile protonation of NH_2 groups, tren-based small-molecule fluorophores are water-soluble. In 2013, Gunnlaugsson *et al.* synthesized an interesting 4-amino-1,8-naphthalimide-based fluorescence sensor **Nap-11** functionalized with a tren receptor moiety at the 4th position of the naphthalimide moiety (Fig. 9).[39] The sensor **Nap-11** exhibited an efficient and selective fluorescence quenching of up to 80% and a blue shift in the absorption band upon the addition of Cu(II) ions in 100 mM NaCl buffer solution. Further studies demonstrated that the fluorescence emission properties altered with a change in the pH of the solution. This is because the tren-receptor NH_2 groups are involved in the PET process thereby quenching the fluorescence intensity in the basic pH. Meanwhile in acidic pH < 4, the NH_2 groups are protonated which inhibits the PET process and thus enhances the fluorescence emission. The observed fluorescence changes in response to the change in pH of the medium were found to be fully reversible. At a highly acidic pH, the binding ratio between Cu(II) and **Nap-11** was 1 : 2, but this ratio changed to a 1 : 1 at physiological pH. In addition to the excellent sensing characteristics, sensor **Nap-11** can be easily recovered from the metal–sensor complex upon titrating with the chelating agent EDTA or glutathione.

In 2019, Qian and team designed and synthesized a series of amino-1,8-naphthalimide-based fluorescence sensors (**Nap-12** to **Nap-15**) for multiple applications, of which Cu(II) ion sensing is one of the main purposes (Fig. 10A).[40] Upon screening the selectivity of these sensors towards various metal ions in the Tris-HCl buffer medium, the emission characteristics displayed an efficient and selective quenching for Cu(II) ions. The sensors **Nap-12** to **Nap-15** exhibited almost 116, 20, 12, and 14-fold quenching of emission intensity with the addition of 5-equivalents of Cu(II) ions, respectively. Interestingly, similar studies with other metal ions showed no notable fluorescence changes, except a one-fold emission enhancement observed for sensor **Nap-14** upon the addition of Fe(III) ions. It was suggested that the possible reason for this is due to the peculiar structural features of **Nap-14** compared to other sensors. Furthermore, the

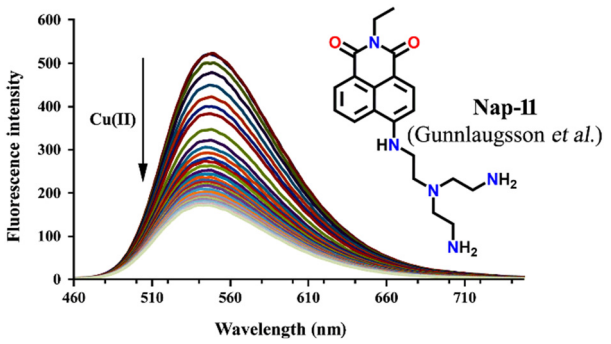

Fig. 9 The changes in ICT-based fluorescence emission spectra of **Nap-11** as a function of increasing concentration of Cu(II) upon excitation at λ = 445 nm (inset: the structure of sensor **Nap-11**). Reproduced with permission from ref. 39. Copyright 2013 Taylor and Francis.

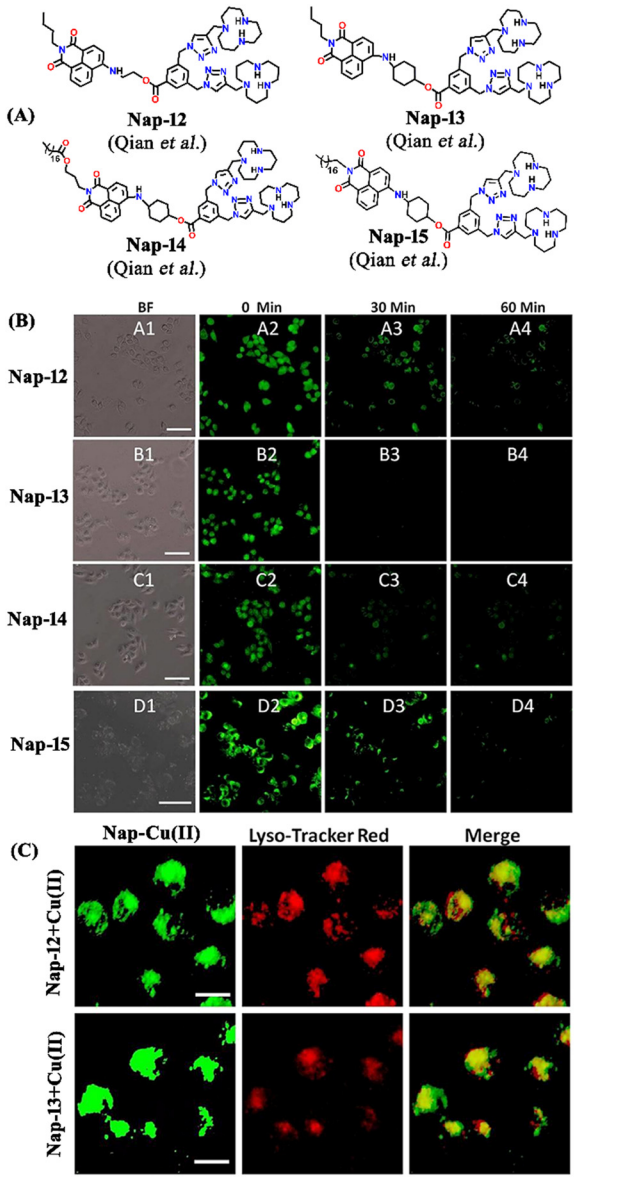

Fig. 10 (A) The structure of sensors **Nap-12** to **Nap-15**. (B) Confocal fluorescence microscopy images of HeLa cells treated with sensors **Nap-12** to **Nap-15** and then incubated with Cu(II) ions (the images were recorded at different times). (C) Fluorescence microscopy images of HeLa cells incubated with **Nap-12** + Cu(II) and **Nap-13** + Cu(II) complexes and Lyso-Tracker red for 0.5 h. Reproduced with permission from ref. 40. Copyright 2019 Frontiers.

presence of a long hydrophobic chain as well as the carbonyl group attached to the 1,8-naphthalimide moiety restricted the PET process and thereby enhanced the fluorescence emission intensity. The detection limit of **Nap-12** to **Nap-14** was estimated to be 2.62×10^{-9}, 4.51×10^{-9}, and 1.17×10^{-8} M, and Job's plot confirmed the binding ratio between sensors and Cu(II) to be 1:2. The paramagnetic nature of Cu(II) ions and the effective coordination of the amino group towards Cu(II) ions leads to excellent fluorescence quenching properties. Along with Cu(II) sensing in a buffer medium, cellular imaging studies were also performed using HeLa cells. Sensors **Nap-12** to **Nap-15** were highly emissive within HeLa cells and the subsequent incubation of Cu(II) quenched the fluorescence emission (Fig. 10B). This was further extended to demonstrate the use of sensor-Cu(II) complexes to visualize them within the lysosomes in live HeLa cancer cell lines (Fig. 10C). All these studies demonstrated that triazole-based ligands **Nap-12** to **Nap-15** could be used as potential fluorescence sensors for the trace determination of Cu(II) both in the buffer medium and within the cancer cell lines.

Another interesting fluorescence sensor was reported by Yoon and co-workers, who designed two different 4,5-disubstituted-1,8-naphthalimide sensors, **Nap-16** and **Nap-17**, which showed excellent fluorescence sensing of Cu(II) (Fig. 11A).[41] The fluorescence titration studies using **Nap-16** and **Nap-17** in HEPES buffer solutions (0.5 M, pH = 7.4) displayed unique alteration with the addition of Cu(II) ions. The broad emission peak of **Nap-16** at λ = 534 nm decreased in intensity which was accompanied by the generation of a blue-shifted emission band at λ = 478 nm upon titrating with Cu(II) ions. These changes indicated the complexation of Cu(II) ions with sensor **Nap-16**. Job's plot confirmed a 1:1 binding ratio between **Nap-16** and Cu(II) ions. The association constant was estimated to be 2.7×10^5 M^{-1} and the limit of detection was 1.0×10^{-8} M^{-1}. Similarly, with the addition of Cu(II) ion solution, sensor **Nap-17** displayed an efficient quenching pattern at λ = 550 nm, and the dissociation constant was calculated to be 2.2×10^{-6} M^{-1}. Upon the interaction with the Cu(II) ion, the NH proton of **Nap-17** gets easily deprotonated which facilitated the observed fluorescence quenching. The absorption spectra of **Nap-17** showed a decrease in the band at λ = 459 nm and the generation of two different bands at λ = 306 and 504 nm which displayed sharp isosbestic points at λ = 390 and 492 nm, respectively. The hypsochromic shift in the fluorescence peak was due to the partial positive charge near the cation because of the interaction of the metal cation with the electron-rich moiety of the fluorophore. Therefore, **Nap-16** can be a ratiometric sensor and **Nap-17** a colorimetric sensor for Cu(II) ion detection. Moreover, the fluorescence sensing responses can be reversed by titrating with CN^- ions, which breaks the coordination complex by forming an effective complex with the Cu(II) ion (Fig. 11B). This reversible switching was reflected by the color changes of both sensors. Therefore, both **Nap-16** and **Nap-17** can be utilized as possible reversible fluorescence and colorimetric sensors for the detection of Cu(II) ions.

A cleft-shaped sensor **Nap-18** was developed by a simple naked-eye substitution reaction between *N*-butyl-4-bromo-5-nitro-1,8-naphthalimide and *N*-phenyl ethylenediamine yielding the expected sensor molecule in analytically pure form and high yield.[42] **Nap-18** was successfully utilized for selective detection of Cu(II) ions, producing clear naked eye color changes (Fig. 12). The yellow color of **Nap-18** changed to pink upon complex formation with Cu(II) ions. Notably, the fluorescence emission of **Nap-18** was observed to be red-shifted from green to red upon binding with the Cu(II) ion (Fig. 12). It was suggested that the reason for the observed sharp color changes might be due to the Cu(II)-coordinated deprotonation of amine groups on the naphthalene ring. It was further proposed that the binding of Cu(II) with **Nap-18**

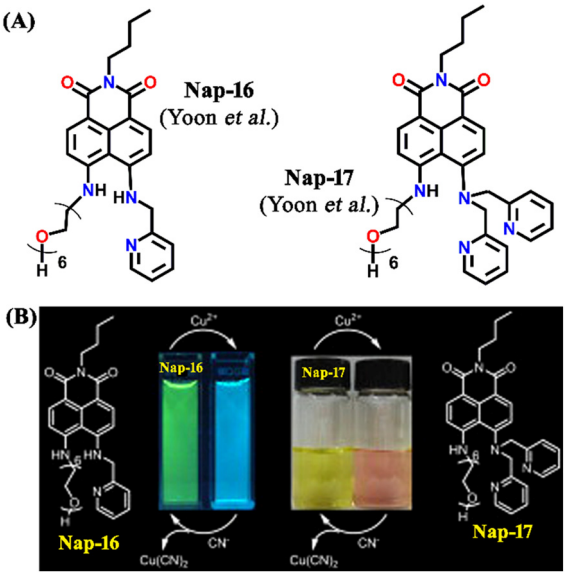

Fig. 11 (A) The structure of sensors **Nap-16** and **Nap-17**. (B) Reversible colorimetric responses of sensors **Nap-16** and **Nap-17** before and after mixing of CN^- ions to their respective Cu(II) complexes. Reproduced with permission from ref. 41. Copyright 2010 Elsevier.

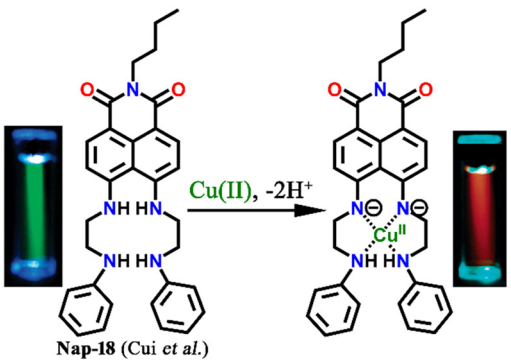

Fig. 12 The structure of sensor **Nap-18** and its Cu(II) complex, and sharp visual changes from green to pink. Reproduced with permission from ref. 42. Copyright 2005 American Chemical Society.

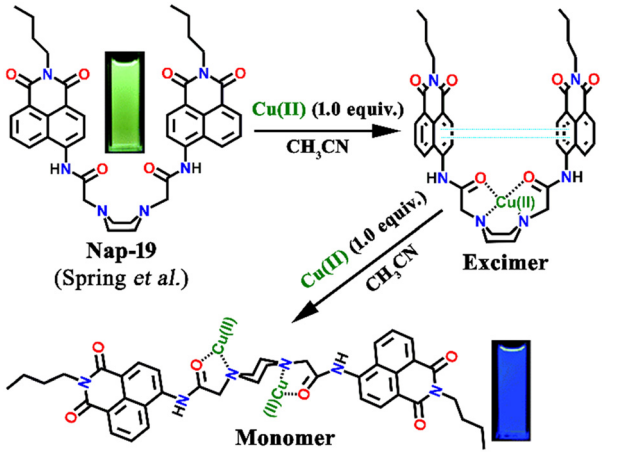

Fig. 13 The proposed Cu(II) sensing mechanism of excimer–monomer switching of sensor **Nap-19** (inset: visual color changes of the sensor from green to blue after complexation with metal) in an aqueous medium. Reproduced with permission from ref. 43. Copyright 2010 Royal Society of Chemistry.

took place in a stepwise manner, first forming a 1:1 complex, then forming a 1:2 complex, and later rapidly releasing two amino protons from the naphthalimide moiety to form the 1:1 chelate complex of **Nap-18** with Cu(II). The observed sharp visual color changes make **Nap-18** a suitable colorimetric and ratiometric probe for Cu(II) ion sensing.

Spring *et al.* designed a unique ratiometric fluorescence sensor **Nap-19** for Cu(II) detection by the incorporation of a piperazine ring into two *N*-butyl-4-acetamido-1,8-naphthalimide moieties (Fig. 13).[43] Upon changing the polarity of the sensing medium from low to high, the piperazine ring of the sensor exhibited a conformational switching from chair to boat, leading to the transformation of 1,8-naphthalimide monomer emission at λ = 450 nm *via* a static excimer formation which emits at λ = 550 nm. Fluorescence emission intensity displayed no noticeable changes with the addition of less than one equivalent of Cu(II) ion, whereas the UV-vis spectra exhibited a notable decrease in peak intensity along with a red-shift as well as peak broadening when one equivalent of Cu(II) ion was added to the sensor solution. However, the second equivalent of Cu(II) ion addition resulted in an enhanced blue shift of the peak. The excited state of the naphthalimide dimer unit induces a dynamic excimer emission in polar solvents in their free state. However, upon complexation with the Cu(II) ion, the obtained complex exhibits a static excimer emission which originated from the ground state of the naphthalimide dimer formation. Further, the bathochromic shift of the excitation spectrum of the complex also validates the formation of the static excimer. In a nutshell, **Nap-19** can be utilized as a ratiometric fluorescence probe for selective sensing of Cu(II) ions in an aqueous solution based on the excimer–monomer switching characteristics of the 1,8-naphthalimide moiety.

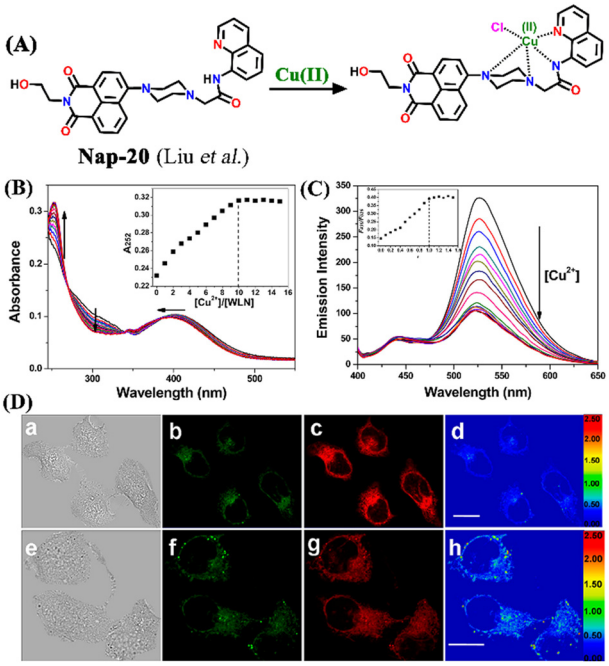

Fig. 14 (A) The structure of sensor **Nap-20** and its Cu(II) complex. (B) The observed changes in the absorption spectra for **Nap-20** after adding Cu(II) solutions (inset: the titration profile based on the absorbance at 252 nm). (C) The relative changes in the fluorescence emission intensity for **Nap-20** upon mixing the Cu(II) ion solution (inset: the obtained titration profile based on the intensity ratio at 435 and 526 nm). (D) The confocal fluorescence image of MCF-7 cells treated with **Nap-20** (above) and subsequent addition of Cu(II) ions (below) (labels a–h are part of the original images). Reproduced with permission from ref. 44. Copyright 2012 American Chemical Society.

Another interesting ratiometric Cu(II) sensor, **Nap-20**, was devised by linking 4-amino-1,8-naphthalimide and 8-aminoquinoline fluorophores through a piperazine linker unit (Fig. 14A).[44] Due to the large spectral overlap, both these fluorophores were excited at the same wavelength. In the HEPES buffer medium, **Nap-20** showed two strong absorption peaks, a peak centered at λ = 252 nm which corresponds to the π–π^* transition, and an ICT-based transition peak at λ = 403 nm (Fig. 14B).

Interestingly, upon incremental addition of Cu(II) ions, **Nap-20** showed a ratiometric response. The absorption intensity of the peak at 252 nm enhanced gradually while the peak at 403 nm slightly blue-shifted and the intensity of the peak was decreased. Similarly, the fluorescence emission spectrum of **Nap-20** showed two intense peaks at λ = 435 and 526 nm; these emission peaks correspond to two different fluorophores of **Nap-20.** The increased addition of Cu(II) ions into the sensor solution induced selective quenching of the emission at 526 nm with no significant changes at 435 nm (Fig. 14C). The ratio between the two emission peaks demonstrated linearity up to 1:1 concentration of **Nap-20** and Cu(II). It was noticed that the observed ratiometric fluorescence response was not altered by the presence of other competing metal cations. Further biological studies of live MCF-7 cell imaging indicated the use of **Nap-20** as a

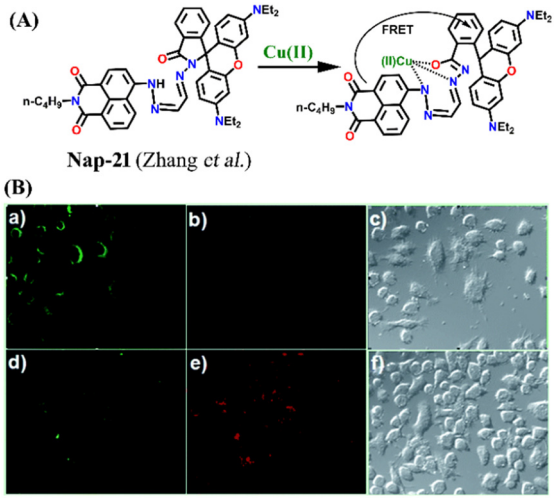

Fig. 15 (A) The structure of sensor **Nap-21** and its Cu(II) complex. (B) The confocal fluorescence images of RAW cells treated with **Nap-21** (top panel) and cells incubated with **Nap-21** and Cu(II) (bottom panel) (labels a–f are part of the original images). The rightmost images are bright-field images. Reproduced with permission from ref. 45. Copyright 2014 Royal Society of Chemistry.

potential ratiometric fluorescence sensor for trace monitoring the Cu(II) ion concentration within the cellular medium (Fig. 14D).

In 2014, Zhang *et al.* reported a unique Cu(II) ion sensor (**Nap-21**) based on an intramolecular fluorescence resonance energy transfer (FRET) mechanism using an amino-1,8-naphthalimide fluorophore which connected through a spacer with a rhodamine B fluorophore (Fig. 15A).[45] The absorption peak of ring-opened rhodamine B at λ = 556 nm significantly overlaps with the emission spectrum of the amino-1,8-naphthalimide which emits at λ = 525 nm which engenders the sensor **Nap-21** to exhibit FRET. The strong emission of **Nap-21** emanating from the amino-1,8-naphthalimide moiety was quenched and a new emission peak at λ = 580 nm was observed in the presence of Cu(II) ions. The appearance of a new peak was assigned to the ring-opening of the spirolactam to form an amide. The detection limit was calculated to be 0.25 μM. Job's plot indicated the formation of a 1:1 metal–ligand coordination complex, which was further validated by ESI-MS analysis. The confocal microscopy images revealed the potential use of **Nap-21** as a ratiometric Cu(II) sensor with high-level practical feasibility (Fig. 15B).

Two structurally similar fluorophore–spacer–receptor types of sensors **Nap-22** and **Nap-23** were configured based on 4-amino-2,2,6,6-tetramethyl piperidinyl for fluorescence sensing of Cu(II) ions (Fig. 16).[46] Among the various metal ions tested Pb(II), Zn(II), and Ni(II), the highest fluorescence enhancement was measured for Cu(II) ions. The fluorescence titration profile indicated a 1:1 complex formation of the sensor with Cu(II) ions. It was proposed that the Cu(II) ions coordinated with both the piperidine moiety and the aromatic amine site which resulted in the restriction of the PET process from the amine receptor site to the 1,8-naphthalimide moiety. Subsequently, the inhibition of PET resulted in an efficient fluorescence enhancement. In addition to the emission enhancement, the chelation of the sensor led to the hypsochromic shift in wavelength due to the reduction in the electron-donating ability of aromatic amine. These studies demonstrated the ability of **Nap-22** and **Nap-23** as efficient fluorescence switches for excellent sensing of Cu(II) ions. These studies were further explored by the same group and in continuation, two more sensors **Nap-24** and **Nap-25** with similar sensing properties were reported (Fig. 16).[47] Sensors **Nap-24** and **Nap-25** were weakly emissive due to the PET process which quenches the intrinsic emission of sensors. But, the coordination of Cu(II) ions with sensors engenders an efficient emission increase due to the prevention of the PET process. Besides Cu(II) sensing, the fluorescence switching of these sensors based on H^+ ion concentrations in solution was demonstrated.

In 2014, Xu and team designed a novel 4-amino-1,8-naphthalimide-based fluorescence sensor **Nap-26** consisting

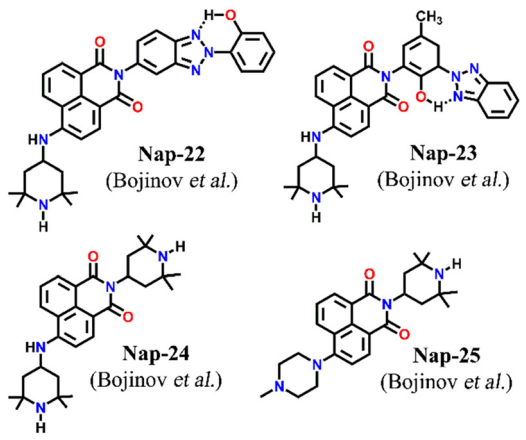

Fig. 16 The structures of sensors **Nap-22** to **Nap-25** employed for selective and efficient sensing of Cu(II) ions.

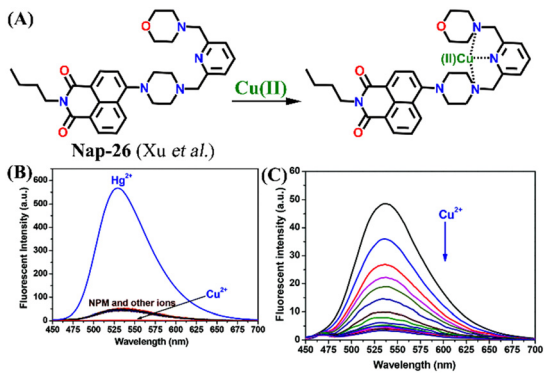

Fig. 17 (A) The structure of sensor **Nap-26** and its Cu(II) coordination complex. (B) The relative changes in fluorescence emission for **Nap-26** in the presence of different metal cations. (C) The observed changes in emission intensity upon the gradual addition of Cu(II) ion solution. Reproduced with permission from ref. 48. Copyright 2014 Royal Society of Chemistry.

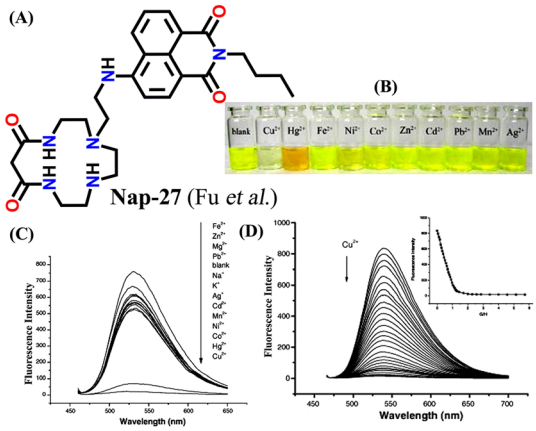

Fig. 18 (A) The structure of sensor **Nap-27** and (B) visual color changes were observed for **Nap-27** before and after mixing with different metal ion solutions. (C) Relative changes in emission intensity upon the addition of various metal ions. (D) The fluorescence titration studies for **Nap-27** at different concentrations of Cu(II) ion solution (inset: a plot of fluorescence changes *vs.* equivalents of Cu(II) ion). Reproduced with permission from ref. 49. Copyright 2007 Elsevier.

of the morpholine moiety as a receptor site for Cu(II) binding (Fig. 17A).[48] **Nap-26** exhibited an efficient fluorescence turn-on sensing response for the Hg(II) ion and a fluorescence turn-off response for Cu(II) in aqueous solution (Fig. 17B). Notably, the observed fluorescence changes gave a linear curve with increasing concentration of metal ions, and the efficient fluorescence quenching in the presence of Cu(II) was attributed to the heavy atom effect (Fig. 17C). Therefore, **Nap-26** can be a potential bifunctional sensor system for the quantification of metal-ion concentrations in solutions.

In 2007, Fu *et al.* reported a novel two-channel fluorescence sensor **Nap-27** designed from macrocyclic dioxotetramine, which acts as a receptor and amino-1,8-naphthalimide (Fig. 18A).[49] The initial emission intensity of **Nap-27** was perturbed upon the addition of Cu(II) and Hg(II) metal ions, while other metal ions showed almost no changes in the emission spectra of **Nap-27** (Fig. 18B). From the titration profile, the limit of detection was found to be 3×10^{-7} M for Cu(II) and 7×10^{-7} M for Hg(II). The observed photophysical changes were also reflected by sharp visual color changes (Fig. 18C). Therefore, **Nap-27** can be utilized as a potential visual and optical sensor for the trace sensing of both Cu(II) and Hg(II) even in the presence of other competing metal cations.

3. Conclusions and outlook

The design and development of suitable chemical sensors for selective detection and ultra-trace monitoring of the concentrations of biologically important analytes and environmentally concerning pollutants have attracted substantial research attention in the past decades. In particular, small-molecule-based chemosensors received special attention because of their easy synthesis, product scalability, facile structures & functional tunability, and high solution processability which facilitates their easy device fabrication. A myriad of small-molecule chemosensors based on different fluorophores have been designed and employed as fluorescence sensors for sensing anions, cations, small molecules, chemical explosives, and biomolecules. Given the facile synthesis, strong absorption & fluorescence emission in the visible region, large Stokes shift, high fluorescence quantum yield, and good photostability, amino-1,8-naphthalimide (**Nap**) derivatives have been extensively used as fluorescence chemosensors for the detection of different metal cations in solutions.

In this article, we have exemplified various examples of **Nap**-based small-molecule fluorescence chemosensors reported to date for the selective sensing and bioimaging of Cu(II) ions. The fluorescence sensing properties of different sensors highlighted in this article are presented in Table 1. We have discussed in detail the photophysical properties, the mode of binding, the fluorescence sensing mechanism, and the bioimaging applications of several sensors for the detection of Cu(II) ions. Gratifyingly, a few of the **Nap** sensors presented in this article exhibited excellent chemical stability under various experimental conditions and high selectivity for selective sensing of Cu(II) even in competitive environments. Hence, **Nap**-based fluorescence sensors have unlimited potential to be used as fluorescence sensors for sensing and bioimaging Cu(II) ions. However, there are multiple issues with **Nap** sensors exemplified in this article and these issues must be resolved for developing practically useful fluorescence sensor systems. Most of the **Nap** sensors reported to date are either fully water-insoluble or partially soluble in water and thus they are not biocompatible. Moreover, the fluorescence sensing studies of **Nap** sensors were largely performed in an organic solvent or in a mixture of organic solvent and H_2O medium, which limits their bio-imaging applications. Therefore, developing water-soluble **Nap** fluorescence sensors for Cu(II) sensing is imperative.

One feasible method to enhance the water solubility of **Nap** derivatives is to functionalize the sensors with water-soluble organic ligands. In light of this, Gunnlaugsson *et al.* have synthesized a **Nap**-based fluorescence sensor functionalized with tris(2-aminoethyl)amine (TREN) chelating amine, which enhanced the water solubility of **Nap** sensors and also acts as a receptor site forming a stable coordination complex with metal cations.[39] One such example is sensor **Nap-11** substituted with the TREN ligand at the imide site, which was found to be fully soluble in water and forms a stable 2:1 selective coordination complex with Cu(II) ions in water. In this direction, further work is in progress in our group for developing biocompatible and practically useful **Nap**-based fluorescence sensors for sensing and bioimaging of biologically relevant metal cations.

As alluded to above, **Nap** derivatives are strongly colored and they absorb and emit in the visible region. For *in vivo*

Table 1 Summary of the fluorescence sensing properties of different **Nap**-based fluorescence chemosensors for Cu(II) ions

Structure of sensor	Emission maxima, λ_{max} (nm)	Sensing medium	Selectivity	K_{SV} or K_a	Sensitivity/LoD	Sensing mechanism/fluorescence responses	Ref.
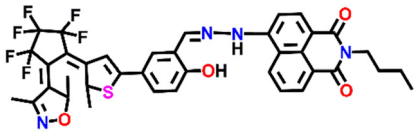 **Nap-1**	542	CH_3CN	Cu(II)	3.13×10^4 L mol^{-1}	2.4×10^{-6} mol L^{-1}	Inhibition of ICT/turn-off	29
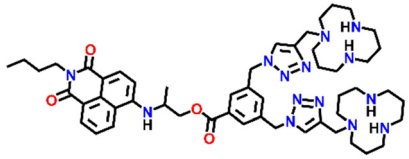 **Nap-2**	541	Tris-HCl buffer	Cu(II)	—	1.3×10^{-8} M	Non-radiative decay/turn-off	30
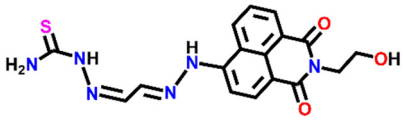 **Nap-3**	530	CH_3CN/H_2O	Cu(II)	—	0.0326 μM	Suppression of excited quenching/turn-on	31
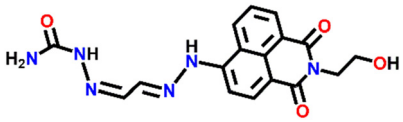 **Nap-4**	—	CH_3CN/H_2O	Cu(II)	—	—	Suppression of excited quenching/turn-on	31
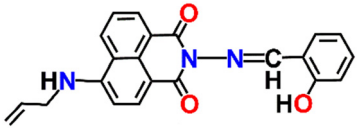 **Nap-5**	539	Tris-HCl buffer	Cu(II)	1.088×10^6 M^{-1}	0.32 μM	—/turn-off	32
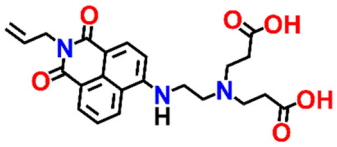 **Nap-6**	532	DMSO–HEPES buffer	Cu(II)	1.14×10^6 M^{-1}	4.67×10^{-8} M	—/turn-off	33

Table 1 *(continued)*

Structure of sensor	Emission maxima, λ_{max} (nm)	Sensing medium	Selectivity	K_{SV} or K_a	Sensitivity/LoD	Sensing mechanism/fluorescence responses	Ref.
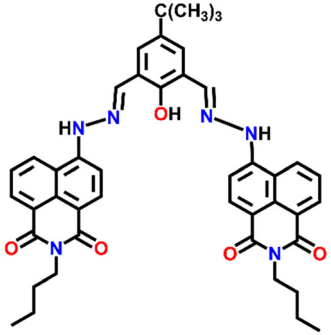 Nap-7	560	CH_3CN/H_2O	Cu(II)	$1.58 \pm 0.45 \times 10^9$ M^{-2}	64 ppb	PET/turn-off	34
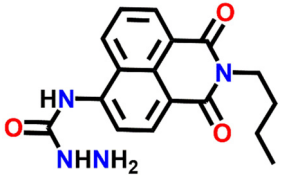 Nap-8	532	Buffer water/CH_3CN	Cu(II)	—	5.2×10^{-8} mol L^{-1}	Cu(II) ion-promoted hydrolysis/turn-on	35
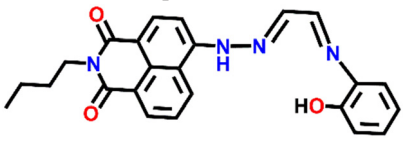 Nap-9	519	CH_3CN/H_2O	Cu(II)	1.1×10^{10} M^{-1}	0.15 μM	Inhibition of PET/turn-on	36
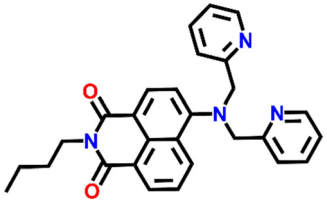 Nap-10	527	CH_3CN/H_2O	Cu(II)	4.5×10^4 M^{-1}	—	Suppression of ICT/turn-off	37
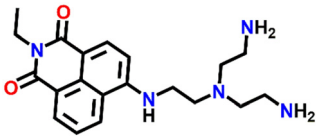 Nap-11	545	Buffered 100 mM NaCl solution	Cu(II)	$\log\beta_{2:1} = 6.46$ (±0.08) and $\log\beta_{1:1} = 6.23$ (±0.11)	—	PET/turn-off	39

Table 1 *(continued)*

Structure of sensor	Emission maxima, λ_{max} (nm)	Sensing medium	Selectivity	K_{SV} or K_a	Sensitivity/LoD	Sensing mechanism/fluorescence responses	Ref.
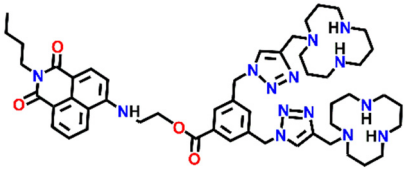 Nap-12	541	Tris-HCl buffer	Cu(II)	—	2.62×10^{-9} M	Restricted PET process/turn-on	40
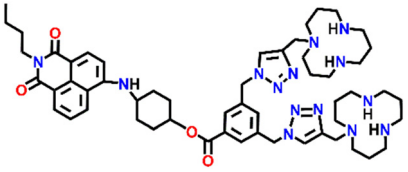 Nap-13	546	Tris-HCl buffer	Cu(II)	—	4.51×10^{-9} M	Restricted PET process/turn-on	40
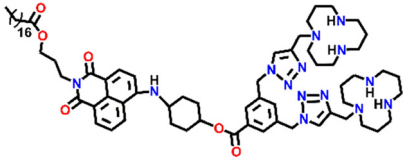 Nap-14	540	Tris-HCl buffer	Cu(II)	—	1.17×10^{-8} M	Restricted PET process/turn-on	40
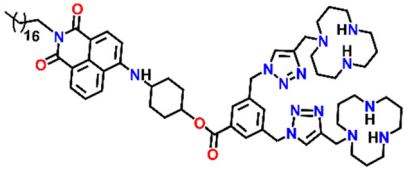 Nap-15	536	Tris-HCl buffer	Cu(II)	—	—	Restricted PET process/turn-on	40
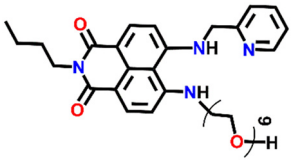 Nap-16	534	HEPES buffer	Cu(II)	2.7×10^{-5} M^{-1}	1.0×10^{-8} M	NH-deprotonation/turn-off	41
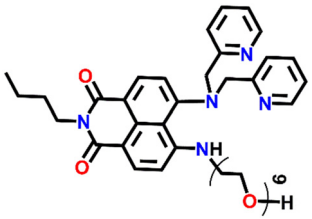 Nap-17	550	HEPES buffer	Cu(II)	2.2×10^{-6} M^{-1}	1.0×10^{-9} M	NH-deprotonation/turn-off	41

Table 1 *(continued)*

Structure of sensor	Emission maxima, λ_{max} (nm)	Sensing medium	Selectivity	K_{SV} or K_a	Sensitivity/LoD	Sensing mechanism/fluorescence responses	Ref.
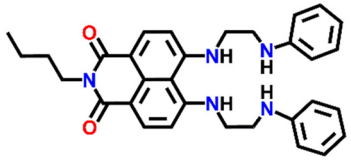 Nap-18	518	Ethanol–H_2O	Cu(II)	—	—	Cu(II)-coordinated deprotonation/shift-in wavelength	42
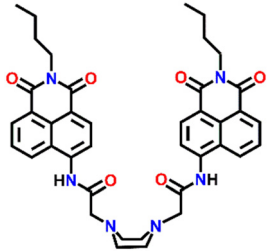 Nap-19	450	CH_3CN/HEPES buffer	Cu(II)	2.94×10^5 M^{-1}	—	Excimer–monomer switching/wavelength shift	43
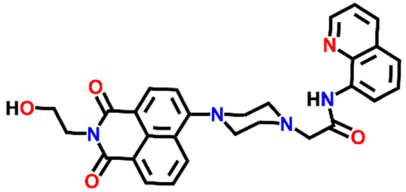 Nap-20	526	HEPES buffer	Cu(II)	2.9×10^4 M^{-1}	—	Ratiometric fluorescence sensing/turn-off	44
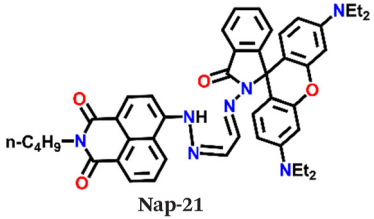 Nap-21	525	Ethanol/H_2O	Cu(II)	—	0.25 mM	FRET/turn-off	45
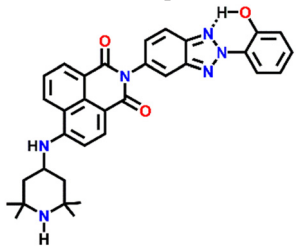 Nap-22	541	H_2O/DMF	Cu(II), Pb(II), Zn(II), Ni(II) and protons	—	—	Inhibition of PET/turn-on	46

Table 1 *(continued)*

Structure of sensor	Emission maxima, λ_{max} (nm)	Sensing medium	Selectivity	K_{SV} or K_a	Sensitivity/LoD	Sensing mechanism/fluorescence responses	Ref.
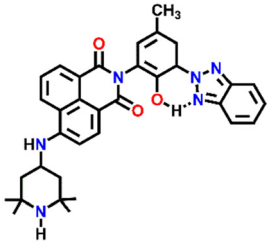 Nap-23	542	H_2O/DMF	Cu(II), Pb(II), Zn(II), Ni(II) and protons	—	—	Inhibition of PET/turn-on	46
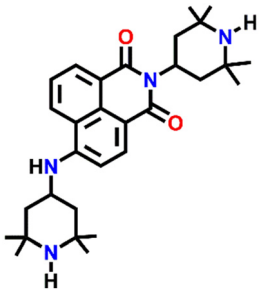 Nap-24	539	DMF and H_2O	Cu(II), Pb(II), Zn(II), Ni(II), Co(II) and protons	—	—	Inhibition of PET/turn-on	47
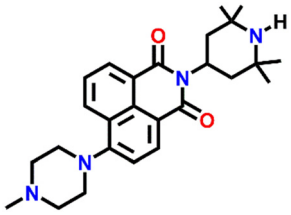 Nap-25	534	DMF and H_2O	Cu(II), Pb(II), Zn(II), Ni(II), Co(II) and protons	—	—	Inhibition of PET/turn-on	47
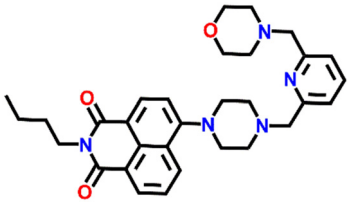 Nap-26	529	HEPES buffer	Cu(II), Hg(II)	3.51×10^6 M^{-1}	—	Heavy atom effect/turn-off	48
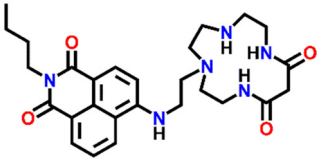 Nap-27	538	H_2O/CH_3OH	Cu(II), Hg(II)	10 074 M^{-1}	3×10^{-7} M	—/turn-off	49

bioimaging applications, sensors with fluorescence emission in the red and near-infrared region are highly preferable. Therefore, further structure and functional modifications of **Nap**-based sensors are essential for real-time sensing and imaging of Cu(II) within biological systems. Another issue with **Nap** sensors is their poor sensitivity for target analyte detection. Compared to conjugated polymer-based fluorescence sensors, discrete small-molecule fluorophores have less sensitivity because of their stochiometric binding with target analytes. Most of the **Nap** sensors discussed herein sense Cu(II) ions at higher levels than the permissible concentrations of metal cations in groundwater and biological systems. The sensitivity of **Nap**-based small molecule fluorescence sensors can be improved by connecting discrete fluorophores into supramolecular polymeric sensors *via* a molecular self-assembly process. This can be achieved by attaching self-assembling functional groups such as COOH, OH, and NH_2 on the periphery of the **Nap** unit.[50] The supramolecular self-assembly is a promising one-step synthetic method used to design the targeted products in quantitative yield.[51] Recently, this strategy has been successfully used to develop various supramolecular polymeric fluorescence sensors for the sensitive detection of secondary chemical explosives.[1] The enhanced sensitivity is ascribed to the molecular wire effect, where the fluorescence quenching is communicated *via* long-range excitonic migration along the polymeric chains. Therefore, **Nap** derivatives can be used as a lead compound to develop fluorescence sensors with superior sensitivity by functionalizing the **Nap** core moiety with desired substituents.

Another issue with **Nap**-based sensors is their poor photostability. **Nap**-derivatives are known to form strong intermolecular π–π stacking interactions between the adjacent units, which in general results in self-quenching of intrinsic fluorescence emission due to the aggregation-caused quenching (ACQ) effect.[52,53] The photostability of **Nap** derivatives can be improved by introducing bulky substituents on the periphery of **Nap** units. The bulky substituents can prevent molecular aggregation and thus retain the intrinsic fluorescence emission of **Nap** fluorophores. The photostability also can be enhanced by immobilizing the **Nap** fluorophores within the polymer-based matrixes like molecularly imprinted polymers having appropriate internal cavities for guest encapsulation. Furthermore, the high selectivity of **Nap** sensors for Cu(II) detection can be achieved by sensibly altering the receptor cavity size to match the size of Cu(II) ions.

In summary, we believe that this review conveys the advantages of **Nap**-based sensors in fluorescent sensing and the importance of Cu(II) sensing and bioimaging applications. We also hope that this review article will be useful to researchers working in related areas and encourage new ideas for the design of reliable chemosensors for Cu(II) detection in the future.

Conflicts of interest

There are no conflicts to declare.

Acknowledgements

The authors are grateful to the Indian Institute of Technology Palakkad (ERG research grant 2023-168-CHY-SHS-ERG-SP to SS), India, for financial support and CIF at the Indian Institute of Technology Palakkad for the facility.

Notes and references

1 S. Shanmugaraju and P. S. Mukherjee, *Chem. Commun.*, 2015, **51**, 16014–16032; P. R. Lakshmi, P. Nanjan, S. Kannan and S. Shanmugaraju, *Coord. Chem. Rev.*, 2021, **435**, 213793–213820.
2 D. Wu, A. C. Sedgwick, T. Gunnlaugsson, E. U. Akkaya, J. Yoon and T. D. James, *Chem. Soc. Rev.*, 2017, **46**, 7105–7123; H. N. Kim, W. X. Ren, J. S. Kim and J. Yoon, *Chem. Soc. Rev.*, 2012, **41**, 3210–3244.
3 S.-H. Park, N. Kwon, J.-H. Lee, J. Yoon and I. Shin, *Chem. Soc. Rev.*, 2020, **49**, 143–179; B. Mohan, M. K. Noushija and S. Shanmugaraju, *Tetrahedron Lett.*, 2022, **109**, 154155.
4 Y. Li, J. Pang and X.-H. Bu, *Chem. Commun.*, 2022, **58**, 7890–7908; Q. Ding, C. Li, H. Wang, C. Xu and H. Kuang, *Chem. Commun.*, 2021, **57**, 7215–7231.
5 Z.-X. Wang and S.-N. Ding, *Anal. Chem.*, 2014, **86**, 7436–7445; R. Verma and B. D. Gupta, *Food Chem.*, 2015, **166**, 568–575.
6 D. Zhu, Y. Luo, X. Yan, W. Xie, W. Cai and X. Zhong, *RSC Adv.*, 2016, **6**, 87110–87114; R. Azadbakht and J. Khanabadi, *Spectrochim. Acta, Part A*, 2014, **124**, 249–255.
7 S. Yin, W. Yuan, J. Huang, D. Xie, B. Liu, K. Jiang and H. Qiu, *Spectrochim. Acta, Part A*, 2012, **96**, 82–88; X. He, J. Zhang, X. Liu, L. Dong, D. Li, H. Qiu and S. Yin, *Sens. Actuators, B*, 2014, **192**, 29–35.
8 H. Kodama and C. Fujisawa, *Metallomics*, 2009, **1**, 42–52; H. Kodama, *Handbook of Copper Pharmacology*, ed. E. Massaro, Human Press, Totowa (USA), 2002, pp. 319–338.
9 P. C. Bull, G. R. Thomas, J. M. Rommens, J. R. Forbes and D. W. Cox, *Nat. Genet.*, 1993, **5**, 327–337.
10 E. Gaggelli, H. Kozlowski, D. Valensin and G. Valensin, *Chem. Rev.*, 2006, **106**, 1995–2044.
11 H. Kodama, Genetic disorders of copper metabolism, in *Toxicology of metals*, ed. L. W. Chang, Lewis Publishers, New York, 1996, pp. 371–385.
12 T. Henson, J. Navratilova, K. Griggs, K. Bradham, K. Rogers and M. Hughes, *Cytotoxicity of copper (II) oxide nanoparticles in rat and human intestinal cell models*, Society of Toxicology, Baltimore, Maryland, March 12–16, 2017.
13 N. Kwon, Y. Hu and J. Yoon, *ACS Omega*, 2018, **3**, 13731–13751; D. Cao, Z. Liu, P. Verwilst, S. Koo, P. Jangjili, J. S. Kim and W. Lin, *Chem. Rev.*, 2019, **119**, 10403–10519.
14 Y. Wang, X. Wang, W. Ma, R. Lu, W. Zhou and H. Gao, *Chemosensors*, 2022, **10**, 399; M. Formica, V. Fusi, L. Giorgi and M. Micheloni, *Coord. Chem. Rev.*, 2012, **256**, 170–192.
15 L. Yang, N. Huang, L. Huang, M. Liu, H. Li, Y. Zhang and S. Yao, *Anal. Methods*, 2017, **9**, 618–624.

16 P. Wainwright, D. Wadey and P. Cook, *Ann. Clin. Biochem.*, 2018, **55**, 485–490.
17 S. S. Alharthi and H. M. Al-Saidi, *Appl. Sci.*, 2020, **10**, 3895.
18 M. Safaei, M. M. Foroughi, N. Ebrahimpoor, S. Jahani, A. Omidi and M. Khatami, *TrAC, Trends Anal. Chem.*, 2019, **118**, 401–425.
19 S. Erbas-Cakmak, S. Kolemen, A. C. Sedgwick, T. Gunnlaugsson, T. D. James, J. Yoon and E. U. Akkaya, *Chem. Soc. Rev.*, 2018, **47**, 2228–2248.
20 T. Gorai, W. Schmitt and T. Gunnlaugsson, *Dalton Trans.*, 2021, **50**, 770–784.
21 Z. Freixa, I. Rivilla, F. Monrabal, J. J. Gómez-Cadenas and F. P. Cossío, *Phys. Chem. Chem. Phys.*, 2021, **23**, 15440–15457; C.-Y. Yao and A. P. de Silva, *ChemPlusChem*, 2022, e202200362.
22 B. Valeur and I. Leray, *Coord. Chem. Rev.*, 2000, **205**, 3–40.
23 A. P. de Silva, H. Q. N. Gunaratne, T. Gunnlaugsson, A. J. M. Huxley, C. P. McCoy, J. T. Rademacher and T. E. Rice, *Chem. Rev.*, 1997, **97**, 1515–1566.
24 R. Gui, H. Jin, X. Bu, Y. Fu, Z. Wang and Q. Liu, *Coord. Chem. Rev.*, 2019, **383**, 82–103.
25 C. Guo, A. C. Sedgwick, T. Hirao and J. L. Sessler, *Coord. Chem. Rev.*, 2021, **427**, 213560.
26 S. Banerjee, E. B. Veale, C. M. Phelan, S. A. Murphy, G. M. Tocci, L. J. Gillespie, D. O. Frimannsson, J. M. Kelly and T. Gunnlaugsson, *Chem. Soc. Rev.*, 2013, **42**, 1601–1618; J. M. Delente, D. Umadevi, S. Shanmugaraju, O. Kotova, G. W. Watson and T. Gunnlaugsson, *Chem. Commun.*, 2020, **56**, 2562–2565.
27 H.-Q. Dong, T.-B. Wei, X.-Q. Ma, Q.-Y. Yang, Y.-F. Zhang, Y.-J. Sun, B.-B. Shi, H. Yao, Y.-M. Zhang and Q. Lin, *J. Mater. Chem. C*, 2020, **8**, 13501–13529.
28 S. A. Murphy, C. Phelan, S. Shanmugaraju, S. Blasco and T. Gunnlaugsson, *Tetrahedron Lett.*, 2021, **77**, 153405; S. Murphy, S. A. Bright, T. McCabe, J. A. Kitchen, E. B. Veale, D. C. Williams and T. Gunnlaugsson, *Org. Biomol. Chem.*, 2014, **12**, 6610–6623.
29 Y. Fu, C. Fan, G. Liu and S. Pu, *Sens. Actuators, B*, 2017, **239**, 295–303.
30 Y.-G. Gao, Q. Tang, Y.-D. Shi, Y. Zhang and Z.-L. Lu, *Talanta*, 2016, **152**, 438–446.
31 J. Chen, W. Su, E. Wang and Y. Liu, *J. Lumin.*, 2016, **180**, 301–305.
32 S. O. Aderinto, Y. Xu, H. Peng, F. Wang, H. Wu and X. Fan, *J. Fluoresc.*, 2017, **27**, 79–87; S. O. Aderinto, *J. Chin. Chem. Soc.*, 2017, **64**, 1432–1445; Y. Xu, S. O. Aderinto, H. Wu, H. Peng, H. Zhang, J. Zhang and X. Fan, *Z. Naturforsch. B*, 2017, **72**, 35–41.
33 G. Huang, C. Li, X. Han, S. O. Aderinto, K. Shen, S. Mao and H. Wu, *Luminescence*, 2018, 1–10; C. Li, X. Han, S. Mao, S. O. Aderinto, X. Shi, K. Shen and H. Wu, *Color. Technol.*, 2018, **134**, 230–239.
34 G. He, Q. Meng, X. Zhao, C. He, P. Zhou and C. Duan, *Inorg. Chem. Commun.*, 2016, **65**, 28–31.
35 X.-X. Hu, X.-L. Zheng, X.-X. Fan, Y.-T. Su, X.-Q. Zhan and H. Zheng, *Sens. Actuators, B*, 2016, **227**, 191–197.
36 Z. Chen, L. Wang, G. Zou, J. Tang, X. Cai, M. Teng and L. Chen, *Spectrochim. Acta, Part A*, 2013, **105**, 57–61.
37 H. Wang, L. Yang, W. Zhang, Y. Zhou, B. Zhao and X. Li, *Inorg. Chim. Acta*, 2012, **381**, 111–116.
38 K. S. Gayen, T. Das and N. Chatterjee, *Eur. J. Inorg. Chem.*, 2021, **2021**, 861–876.
39 E. B. Veale, J. A. Kitchen and T. Gunnlaugsson, *Supramol. Chem.*, 2013, **25**, 101–108.
40 Y.-G. Gao, F.-L. Liu, S. Patil, D.-J. Li, A. Qadir, X. Lin, Y. Tian, Y. Li and A.-R. Qian, *Front. Chem.*, 2019, **7**, 616.
41 Z. Xu, J. Pan, D. R. Spring, J. Cui and J. Yoon, *Tetrahedron*, 2010, **66**, 1678–1683.
42 Z. Xu, X. Qian and J. Cui, *Org. Lett.*, 2005, **7**, 3029–3032.
43 Z. Xu, J. Yoon and D. R. Spring, *Chem. Commun.*, 2010, **46**, 2563–2565.
44 Z. Liu, C. Zhang, X. Wang, W. He and Z. Guo, *Org. Lett.*, 2012, **14**, 4378–4381.
45 C. Yu, Y. Wen, X. Qin and J. Zhang, *Anal. Methods*, 2014, **6**, 9825–9830.
46 V. B. Bojinov and I. P. Panova, *Dyes Pigm.*, 2009, **80**, 61–66.
47 V. B. Bojinov, N. I. Georgiev and P. Bosch, *J. Fluoresc.*, 2009, **19**, 127–139.
48 C.-B. Huang, H.-R. Li, Y. Luoc and L. Xu, *Dalton Trans.*, 2014, **43**, 8102–8108.
49 H. Mu, R. Gong, Q. Ma, Y. Sun and E. Fu, *Tetrahedron Lett.*, 2007, **48**, 5525–5529.
50 P. Vishnoi, S. Sen, G. N. Patwari and R. Murugavel, *New J. Chem.*, 2015, **39**, 886–892.
51 S. Shanmugaraju, A. K. Bar, S. A. Joshi, Y. P. Patil and P. S. Mukherjee, *Organometallics*, 2011, **30**, 1951–1960.
52 X.-M. Sun, J. Liu, Z.-H. Li, Y.-P. Fu, T.-T. Huang, Z.-D. Tang, B. Shi, H. Yao, T.-B. Wei and Q. Lin, *Chin. Chem. Lett.*, 2023, **34**, 107792-1–107792-5.
53 G.-F. Gong, Y.-Y. Chen, Y.-M. Zhang, Y.-Q. Fan, Q. Zhao, J.-N. An, H. Yao, T.-B. Wei and Q. Lin, *ACS Sustainable Chem. Eng.*, 2020, **8**, 5831–5836.